JOURNAL OF AIRCRAFT
Vol. 38, No. 2, March–April 2001

Response Surface Method for Airfoil Design in Transonic Flow

Jaekwon Ahn,* Hyoung-Jin Kim,† Dong-Ho Lee,‡ and Oh-Hyun Rho§
Seoul National University, Seoul 151-742, Republic of Korea

A response surface method (RSM) applied to a transonic airfoil design problem is studied with other optimization methods. The objective function and constraints of RSM are modeled by quadratic polynomials, and the response surfaces are constructed by Navier–Stokes analyses in the transonic flow region. To assess the advantages of RSM, the design results by RSM are compared to those of a gradient-based optimization method (GBOM), namely, the discrete adjoint variable method. Comparisons are made for various sets of design variables and geometric constraints. It is observed that the response surface method is able to capture the nonlinear behavior of the objective function and smooth out high-frequency noises in transonic regime. These features enable the method to design a shock-free transonic airfoil with fewer design variables than in GBOM. In addition, RSM gives robust design results for the geometric constraints with different characteristics, whereas the GBOM depends heavily on the method of constraint specification. The results indicate that RSM could be used as an effective design tool for multidisciplinary design optimization problems, in which flowfields of design conditions are significantly nonlinear with many constraints imposed.

Nomenclature

C_d, C_l	=	aerodynamic coefficients, lift and drag, respectively
$\boldsymbol{E}, \boldsymbol{F}$	=	inviscid flux vectors
$\boldsymbol{E}_v, \boldsymbol{F}_v$	=	viscid flux vectors
J	=	Jacobian
n_{rc}	=	number of regression coefficient
n_s	=	number of observations
n_v	=	number of design variables
$\boldsymbol{Q}$	=	vector of conservative variables
$\boldsymbol{R}$	=	residual vector
t/c	=	thickness-to-chord ratio
w_k	=	weighting factors of shape function
$\boldsymbol{X}$	=	grid position vector
β	=	vector of design variables

Subscripts

p	=	predicted value
0	=	baseline property

Introduction

OBJECTIVE function and constraints in aerodynamic shape optimization involving transonic flow numerical simulation may be nonsmooth and noisy. Nonsmoothness is created by the presence of flow discontinuities such as shock waves. Noise can be caused either by the changes in computational mesh geometry due to free boundaries or by poor convergence of numerical schemes (as occurs when using flux limiters in a shock capturing scheme). Although these features can make a small change in some design parameters, it could lead to a huge ramification in the objective function or constraints. In such a case, it is likely that the design results would fall into just local optima. These issues in transonic flow region are well discussed by Narducci et al.[1]

These nonsmoothness and noise issues of the objective function become more serious in gradient-based optimization methods (GBOMs), where the objective function value as well as its gradient information are used. As the result of a solid mathematical background, GBOMs have been applied to various single disciplinary design problems, including aerodynamic aircraft component design in all subsonic, transonic, and supersonic regimes.[2–4] In multidisciplinary design optimization (MDO) problems, which usually have objective functions coupled with numerous constraints, it is significantly difficult to formulate the design problem with GBOMs. Because the optimization depends greatly on the formulation of the design problem, the process of searching for the optimum is likely to render just a local value. Another shortcoming of GBOMs is that because many analysis programs were not written with an automated design in mind, adaptation of these programs to an optimization code may need significant reprogramming in the analysis routine.

Moreover, additional changes of objectives and constraints require the whole design process to be recalculated with a heavy computational cost.

In light of this, the response surface method (RSM) drew much attention as an efficient tool for the MDO of aerospace vehicles since early 1990s. RSM is advantageous in MDO applications because it provides useful disciplinary models that can be easily combined with each model and manipulated together by designers. Recently, RSM has been successful in combined aerodynamic–structural optimization of the high-speed civil transport design where linear behavior of flow characteristics is dominant.[5,6]

The purpose of this paper is to verify the applicability of RSM in transonic design problems where flow characteristics are highly nonlinear. The validation is performed through quantitative comparisons of the design results with a GBOM using an adjoint variables method. The adjoint variables method[7–10] is chosen because the method makes the computational cost for the gradients of the objective function or constraints independent of the number of the design parameters. The method has, thus, been frequently used as an efficient tool for aerodynamic shape design optimization.

For practical aerodynamic shape design problems, response surface models of polynomial order higher than two are computationally too expensive. RSM, if proven feasible to transonic airfoil design with the quadratic polynomial, is expected to have the following advantages over other direct optimization methods:

1) It smoothes out the high-frequency noise of the objective function and is, thus, expected to find a solution near the global optimum.

2) Various objectives and constraints can be attempted in the design process without additional numerical computations.

3) It can be effectively applied to MDO problems with many objectives and constraints.

4) It does not require a modification in analysis codes.

Received 5 March 2000; revision received 15 August 2000; accepted for publication 11 November 2000.

*Graduate Research Assistant, Department of Mechanical and Aerospace Engineering.

†Senior Researcher, Korea Aerospace Institute.

‡Professor, Department of Mechanical and Aerospace Engineering. Senior Member AIAA.

§Professor, Department of Mechanical and Aerospace Engineering. Senior Member AIAA.

However, there are some drawbacks to RSM. The range of design parameters highly affects the fitting capabilities of the response model. The wide ranges may increase prediction errors such that predicted performances cannot be obtained exactly. RSM also has a limitation on the number of the design parameters because the computation time for construction of the response model is proportional to the square of the number of design parameters.

The objectives of the present paper are as follows: 1) to validate RSM in the transonic turbulent flow region as an aerodynamic design and MDO tool, through comparing the design results with GBOM; 2) to show the effects of the number of design variables on design results, and 3) to compare constraints handling capability of each design method.

To achieve these goals, the same flow analysis code for two-dimensional Navier–Stokes equations is employed in both design methods. During the comparison between RSM and GBOM, the affordable number of design variables is studied with the emphasis on transonic flow applications. Several specifications of geometric constraints are explored for the optimal design.

The following sections briefly describe the technical framework of the flow analysis method and optimization method of GBOM and RSM. Several comparisons of design results are made in the "Results and Discussions" section.

Flow Analysis

A two-dimensional Navier–Stokes solver developed and validated in Refs. 11 and 12 is used for the flow analysis. Reynolds-averaged two-dimensional compressible Navier–Stokes equations in generalized coordinates are used in the conservation form based on a cell-centered finite volume approach,

$$\frac{1}{J}\frac{\partial \boldsymbol{Q}}{\partial t} = -\boldsymbol{R} \tag{1}$$

where $\boldsymbol{Q}$ is a four-element vector of conserved flow variables as $\boldsymbol{Q} = (\rho,\ \rho u,\ \rho v,\ \rho e)^T$ and $\boldsymbol{R}$ is the residual vector as $\boldsymbol{R} = (\boldsymbol{E} - \boldsymbol{E}_v)_\xi + (\boldsymbol{F} - \boldsymbol{F}_v)_\eta$.

Roe's flux difference splitting scheme is adopted for the space discretization in the inviscid flux terms $\boldsymbol{E}$ and $\boldsymbol{F}$ of the residual vector on the right-hand side; the MUSCL approach with a Koren limiter is employed to obtain a third-order accuracy. A central difference method is used for viscous flux terms $\boldsymbol{E}_v$ and $\boldsymbol{F}_v$ of the residual vector. For temporal discretization, a Euler implicit method and linearized van Leer flux Jacobian are used. In the implicit part, Beam and Warming's alternating direction implicit (ADI) method with local time stepping is implemented. Turbulence effects are incorporated using the Baldwin–Lomax algebraic model with a relaxation technique.

A C-type grid system with 169×61 points around an airfoil is generated by a hyperbolic technique. The residual of the flow solver is reduced by four orders of magnitude from the initial condition during the computations of objective function of the GBOM and data point of the RSM.

Design Objective and Variables

The objective of the present design study is to minimize the drag C_d of an airfoil with constraints on lift and contour area or maximum thickness, subject to $C_l - C_{l_0} \geq 0$:

$$\text{Area} - \text{Area}_0 \geq 0 \qquad \text{or} \qquad (t/c) - (t/c)_0 \geq 0 \tag{2}$$

In GBOM, several forms of objective functions and constraints were tested to obtain reasonable design results, from which the following objective function is chosen:

$$F = 10 \cdot C_d + \max\left(C_l - C_{l_0}, 0\right) + 10 \cdot \max(\text{Area} - \text{Area}_0, 0) \tag{3}$$

The penalty factor of 10 is multiplied to balance the orders of magnitude of the terms. When the combined objective function is used, the lift constraint can be slightly violated. If the lift constraint is imposed with a constrained design option in a gradient-based optimizer, excessive computational cost is expected due to the additional adjoint code for the gradient of lift constraint.

The airfoil geometry is modified adding a linear combination of Hicks and Henne shape functions f_k as follows:

$$y - y_{\text{base}} + \sum_{k=1}^{n_v} w_k \cdot f_k, \qquad f_k = \sin^3\left[\pi x^{e(k)}\right]$$

$$e(k) = \frac{\ell n(0.5)}{in(x_k)}, \qquad f_k = \frac{\sqrt{x}(1-x)}{e^{(x \cdot k)}} \tag{4}$$

where x_k represents the location of the maximum height of the base sinusoidal function. Although Hicks and Henne shape functions are not orthogonal functions, the geometry can be highly perturbed at the desirable position by controlling the x_k.

Gradient-Based Optimization with an Adjoint Method

The GBOM in this work couples a computational fluid dynamics (CFD) code and a numerical optimizer to create a design tool. In this study, DOT, a design optimization tool developed by Vanderplaats and Hansen,[13] is adopted. A Broydon–Flectcher–Goldfarb–Shanno variable metric method is selected for unconstrained minimization cases and a modified method of feasible directions is selected for constrained minimization cases.

Sensitivity derivatives are computed by an adjoint sensitivity analysis code developed by Kim et al.,[10] and the code is derived from discrete two-dimensional compressible Navier–Stokes equations with a Baldwin–Lomax algebraic turbulence model.

The discrete residual vector of flow equations for steady problems can be written as

$$\boldsymbol{R}[Q(\beta), X(\beta), \beta] = 0 \tag{5}$$

The design variable β appears in the residual vector explicitly when β is a nongeometric variable such as incidence angle, Mach number, Reynolds number, etc. Equation (5) is directly differentiated with respect to β_k via the chain rule to yield the following equation:

$$\left\{\frac{\mathrm{d}R}{\mathrm{d}\beta_k}\right\} = \left[\frac{\partial R}{\partial Q}\right]\left\{\frac{\mathrm{d}Q}{\mathrm{d}\beta_k}\right\} + \left[\frac{\partial R}{\partial X}\right]\left\{\frac{\mathrm{d}X}{\mathrm{d}\beta_k}\right\} + \left\{\frac{\partial R}{\partial \beta_k}\right\} = 0 \tag{6}$$

The sensitivity derivative of the aerodynamic coefficient C_j with respect to the k-th design variable β_k is given by

$$\frac{\mathrm{d}C_j}{\mathrm{d}\beta_k} = \left\{\frac{\partial C_j}{\partial Q}\right\}^T\left\{\frac{\mathrm{d}Q}{\mathrm{d}\beta_k}\right\} + \left\{\frac{\partial C_j}{\partial X}\right\}^T\left\{\frac{\mathrm{d}X}{\mathrm{d}\beta_k}\right\} + \frac{\partial C_j}{\partial \beta_k} \tag{7}$$

Because the total derivative of the residual vector $\{\mathrm{d}R/\mathrm{d}\beta_k\}$ is null in the steady state, we can introduce the adjoint variable vector and combine Eqs. (6) and (7) to obtain

$$\frac{\mathrm{d}C_j}{\mathrm{d}\beta_k} = \left\{\frac{\partial C_j}{\partial Q}\right\}^T\left\{\frac{\mathrm{d}Q}{\mathrm{d}\beta_k}\right\} + \left\{\frac{\partial C_j}{\partial X}\right\}^T\left\{\frac{\mathrm{d}X}{\mathrm{d}\beta_k}\right\} + \frac{\partial C_j}{\partial \beta_k}$$

$$+ \{\lambda_j\}^T\left\{\left[\frac{\partial R}{\partial Q}\right]\left\{\frac{\mathrm{d}Q}{\mathrm{d}\beta_k}\right\} + \left[\frac{\partial R}{\partial X}\right]\left\{\frac{\mathrm{d}X}{\mathrm{d}\beta_k}\right\} + \left\{\frac{\partial R}{\partial \beta_k}\right\}\right\} \tag{8}$$

Coefficients of the flow variable sensitivity vector $\{\mathrm{d}Q/\mathrm{d}\beta_k\}$ form the following adjoint equation:

$$\left[\frac{\partial R}{\partial Q}\right]^T\{\lambda_j\} + \left\{\frac{\partial C_j}{\partial Q}\right\} = 0 \tag{9}$$

If we find an adjoint variable vector $\{\lambda_j\}$ that satisfies the adjoint equation, we can obtain the sensitivity derivative of C_j with respect to β_k by the following equation, without any information about the flow variable sensitivity vector $\{\mathrm{d}Q/\mathrm{d}\beta_k\}$:

$$\frac{\mathrm{d}C_j}{\mathrm{d}\beta_k} = \left\{\frac{\partial C_j}{\partial X}\right\}^T\left\{\frac{\mathrm{d}X}{\mathrm{d}\beta_k}\right\} + \frac{\partial C_j}{\partial \beta_k} + \{\lambda_j\}^T\left\{\left[\frac{\partial R}{\partial X}\right]\left\{\frac{\mathrm{d}R}{\mathrm{d}\beta_k}\right\} + \left\{\frac{\partial R}{\partial \beta_k}\right\}\right\} \tag{10}$$

This makes the computational cost for sensitivity analysis independent of the number of design variables.

The adjoint equation (9) is converted to a system of linear algebraic equations and is solved by the same ADI scheme as the flow solver. The residual of the adjoint sensitivity analysis code is reduced by four orders of magnitude from an initial value. More details of the adjoint variable method can be found in Ref. 10.

RSM

RSM builds a response model by calculating data points with experimental design theory to prescribe a response of a system with independent variables.[14] The relationship can be written in a general form as follows:

$$y = F\left(x_1, x_2, x_3, x_4, \ldots, x_{n_v}\right) + \varepsilon \tag{11}$$

where ε represents the total error, which is often assumed to have a normal distribution with a zero mean. The response model F is usually assumed as a second-order polynomial, which can be written for n_v variables as follows:

$$y^{(p)} = c_0 + \sum_i c_i x_i + \sum_{1 \le i \le j \le n_v} c_{ij} x_i x_j, \qquad p = 1, \ldots, n_s \tag{12}$$

Basis functions $\varphi_i(x)$ for the regression model of Eq. (12) such as $1; x_1; x_2; x_3, \ldots, x_{nv}; x_1^2, \ldots, x_{nv}^2; x_1x_2; x_1x_3, \ldots, x_1x_{nv}, x_2x_3, \ldots, x_{nv-1}x_{nv}$, lead to an overdetermined matrix problem:

$$\boldsymbol{y} = \boldsymbol{X}\boldsymbol{c} \tag{13}$$

where $\boldsymbol{y} = (y^1, y^2, y^3, \ldots, y^{n_s})$, $\boldsymbol{c} = (c_1, c_2, \ldots, c_{\text{nrc}})$, and $\boldsymbol{X}$ is the $n_s \times n_{\text{rc}}$ matrix, as follows:

$$\boldsymbol{X} = \begin{bmatrix} \varphi_1\left(x^{(1)}\right) & \cdots & \varphi_{\text{nrc}}\left(x^{(1)}\right) \\ \vdots & \ddots & \vdots \\ \varphi_{\text{nrc}}\left(x^{(ns)}\right) & & \varphi_{\text{nrc}}\left(x^{(ns)}\right) \end{bmatrix} \tag{14}$$

As a selection technique of data points, the D-optimality condition[14] is used, and the candidate points are three level factorial designs. The D-optimality criterion states that the n_s points to be chosen are those that maximize the determinant $|\boldsymbol{X}^T\boldsymbol{X}|$. This criterion has following properties:

1) The data point set that maximizes $|\boldsymbol{X}^T\boldsymbol{X}|$ is also the set of points that minimizes the maximum variance of any predicted value from the regression model.

2) The data point set that maximizes $|\boldsymbol{X}^T\boldsymbol{X}|$ is also the set of points that minimizes the variance of the regression coefficients.

3) The design obtained is invariant to changes in scale.

The regression coefficients c_i can be determined using the least-square fitting. The number of regression coefficients (n_{rc}) is $(n_v+1)(n_v+2)/2$ in Eq. (12) and the D-optimal point selection method requires calculating more than n_{rc} data points. It is known to be sufficient to construct a response model with n_s of 1.5~3 times n_{rc} (Ref. 15). In this study, 121 experiments are performed when n_v is 10, and 201 experiments are performed when n_v is 12.

Because the computation time for the construction of the response model is proportional to the square of the number of design variables n_v, RSM has a limitation on the number of design variables. In addition, when an airfoil optimized by RSM is analyzed by a CFD code, one may not obtain the predicted performances because of the intrinsic prediction error of RSM.

Results and Discussion

RAE2822 is selected as the baseline airfoil of the design study. The design condition is imposed as $M_\infty = 0.73$, $\alpha = 2.7$ deg, and $Re = 7 \times 10^6$. RAE2822 exhibits a strong shock on the upper surface under the aforementioned conditions. The lift and drag coefficients of RAE2822 at the design condition are 0.7894 and 0.01928, respectively. The contour area of the airfoil is 0.07780 with a maximum thickness ratio of 0.1210.

Two kinds of design studies are performed to validate the viability of RSM in transonic turbulent flow. First, GBOM with different numbers of design variables are performed to obtain a reference airfoil for RSM. The design results of GBOM are compared to those of RSM with a different number of design variables. Second, two geometric constraints, the area constraint and the maximum thickness constraint, are tested to asses constraint affordability of RSM.

Number of Design Variables

In aerodynamic shape design the real design space is infinite dimensional. The optimum number of design variables may, thus, vary according to the design method and the design problem. Generally, increasing the number of the basis functions may improve the quality of the design.

The method is named depending on the number of design variables in GBOM. For instance, GBO50DV indicates 50 variables design GBOM. Other design cases will also be referred to in similar ways.

To maintain consistency between design variable sets, a design variable set with a larger number of design variables is made by adding new design variables. For example, GBO30DV retains the design variables of GBO20DV and has 10 extra new design variables.

All convergence criteria are used as default values in DOT.[12] However, if the objective value is not improved during four (default value = 2) consecutive design iterations, it is considered to have converged in this work.

Table 1 shows the aerodynamic performances and computing time of optimized airfoils for various GBOMs. The optimized airfoil shapes and corresponding pressure distribution are shown in Fig. 1.

The adjoint code executed to compute the gradients of the objective function requires about twice the CPU time used by the flow solver. For example, the total solver time (24, 2) for GBO10DV in Table 1 implies that the number of flow solver calls and the number of adjoint solver calls is 24 and 2, respectively. This is equivalent to 28 ($=24 + 2 \times 2$) flow solver analyses during the whole optimization process.

The drag coefficients with parentheses in Table 1 are the values when the lift coefficient is 0.7894. These values are acquired using a linear interpolation.

Note from Table 1 and Fig. 1 that the obtained performance and the required computational cost are not proportional to the number of design variables. Because there is much design iteration near the optimum without much change of the objective, there seems to be a higher noise phenomenon of nonsmooth objective function near the optimum.

GBO20DV and GBO30DV with fewer design variables produce better results than GBO40DV. GBO20DV minimizes the drag coefficient from 0.01928 to 0.01545, satisfying the lift coefficient and contour area constraints. However, GBO50DV yields the best performance that has the shock-free airfoil under the contour area and the lift coefficient constraints. The total (pressure plus skin friction) drag coefficient is reduced from 0.01928 to 0.01510. This case can thus be considered as a global optimum for the design problem and the corresponding airfoil is used as a reference airfoil for the following comparisons.

RSMs are then performed with 10 design variables. Figure 2 shows the variation range of design variables for RSM10DV. Table 2 presents the fitting quality of the constructed response models.

Table 1 Aerodynamic performances of optimized airfoils by GBOM

Airfoil	C_l	C_d	L/D	Area	Solver time
RAE2822	0.7894	0.01928	40.94	0.07780	——
GBO10DV	0.7866	0.01573(0.01579)	50.00	0.07781	(24, 2) = 28
GBO20DV	0.7958	0.01545(0.01532)	51.51	0.07898	(53, 9) = 71
GBO30DV	0.7894	0.01544	51.13	0.07783	(111, 24) = 159
GBO40DV	0.7894	0.01570	50.28	0.07811	(96, 20) = 136
GBO50DV	0.7894	0.01510	52.04	0.07785	(146, 32) = 210

Table 2 Fitting quality of RSM10DV

Coefficient	R^2	adjusted-R^2	%RMSE
C_d	0.985	0.968	1.37
C_l	0.998	0.995	0.20

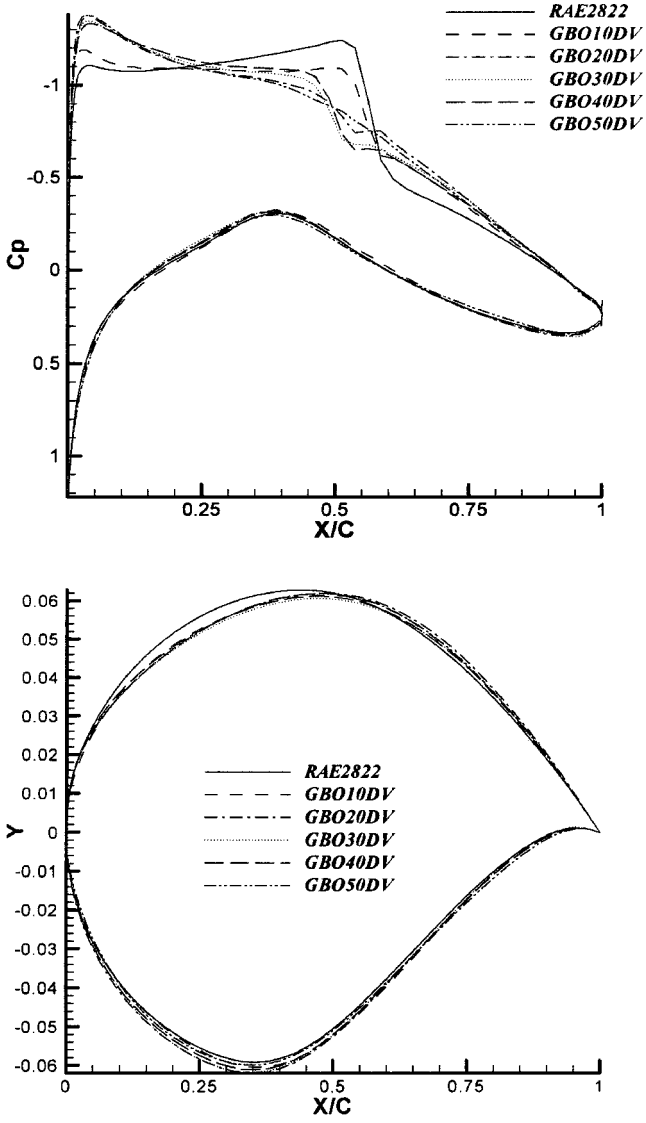

Fig. 1 Airfoil shapes and pressure distribution of GBOMs.

Here, the percentage of root mean square error (%RMSE) is defined as

$$\%\text{RMSE} = 100\sqrt{\frac{1}{n_s}\sum_{i=1}^{n_s}\left(y_1 - y_i^{(p)}\right)^2}\Bigg/\frac{1}{n_s}\sum_{i=1}^{n_s} y_i \qquad (15)$$

R^2, the coefficient of multiple determination, is a measure of the amount of reduction in variability of y obtained by using the regressor variables (design variables) and has the value between 0 and 1. A larger value of R^2 does not necessarily imply that the model is fitted well. Adding a variable to the model always increases R^2, regardless of whether the additional variable is statistically significant or not. Adjusted R^2 is often employed to consider if nonsignificant terms have been included in the model. Because the R^2 and adjusted-R^2 values for C_l and C_d models are larger than 0.96 and %RMSE are less than 1.5%, the response surface models are fitted successfully. Therefore, the quadratic models are sufficient to model the nonsmooth and noisy objective function and the constraints for transonic turbulent flow.

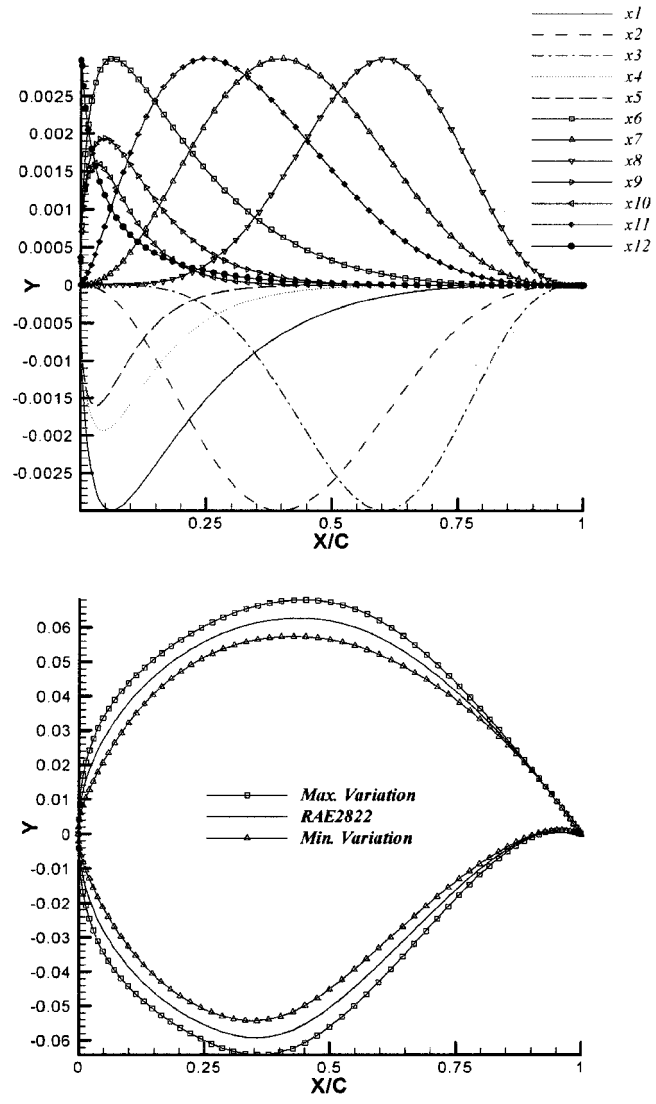

Fig. 2 Used shape functions and range of design variables.

Figure 3 shows the optimized airfoil shapes and surface pressure distributions by both methods. In both methods the shock strengths are reduced and suction peaks somewhat increased. In the case of RSM10DV, the design results are far from the global optimum and are almost similar to those of GBO10DV. When compared to GBO50DV, it is confirmed that RSM10DV has resulted in a local minimum. This is mainly due to the insufficient number of design variables employed. Figure 4 shows the designed airfoil shapes by GBO10DV, RSM10DV, and GBO50DV. Note that 10 design variables are not sufficient to reflect the sharp change of the leading edge shape. This can be seen more clearly by analysis of variance[14] (ANOVA) results on the response surface model presented in Table 3, which shows the results of linear terms of the C_d response model. Here, the t-static is defined as

$$t - \text{static} = \frac{c_{j-1}}{\sqrt{\hat{\sigma}^2 (\boldsymbol{X}^T\boldsymbol{X})^{-1}_{jj}}}, \qquad j = 1, \ldots, N_{\text{rc}} \qquad (16)$$

A higher t-static value means that the term has more dominant effect on the response model than other terms. As shown in Table 3, the design variables $x6$ and $x7$ corresponding to an upper surface leading-edge modification (see Fig. 2) have higher t-static values than others. This strongly implies that we can improve the design results by increasing the variation ranges of $x6$ and $x7$ or by adding more design variables in that region. However, increasing

Table 3 Regression analysis and ANOVA data

Variable	Coefficient	t-static value
$x1$	$-1.217E-04$	-2.886
$x2$	$3.063E-04$	7.232
$x3$	$4.962E-04$	11.482
$x4$	$-1.035E-04$	-2.408
$x5$	$-5.557E-06$	-0.130
$x6$	$9.834E-04$	23.195
$x7$	$1.665E-03$	39.298
$x8$	$-5.907E-04$	-13.818
$x9$	$5.033E-05$	1.202
$x10$	$-2.676E-04$	-6.371

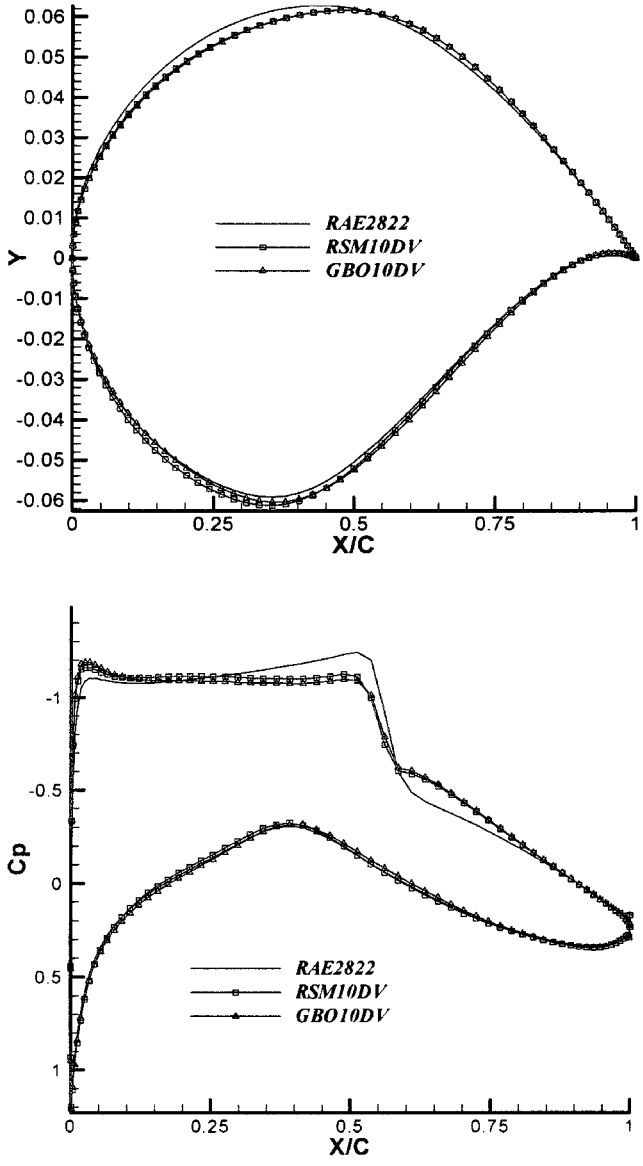

Fig. 3 Design results with 10 design variables.

Table 4 Fitting quality of RSM12DV

Coefficient	R^2	adjusted-R^2	%RMSE
C_d	0.943	0.897	3.39
C_l	0.977	0.958	0.84

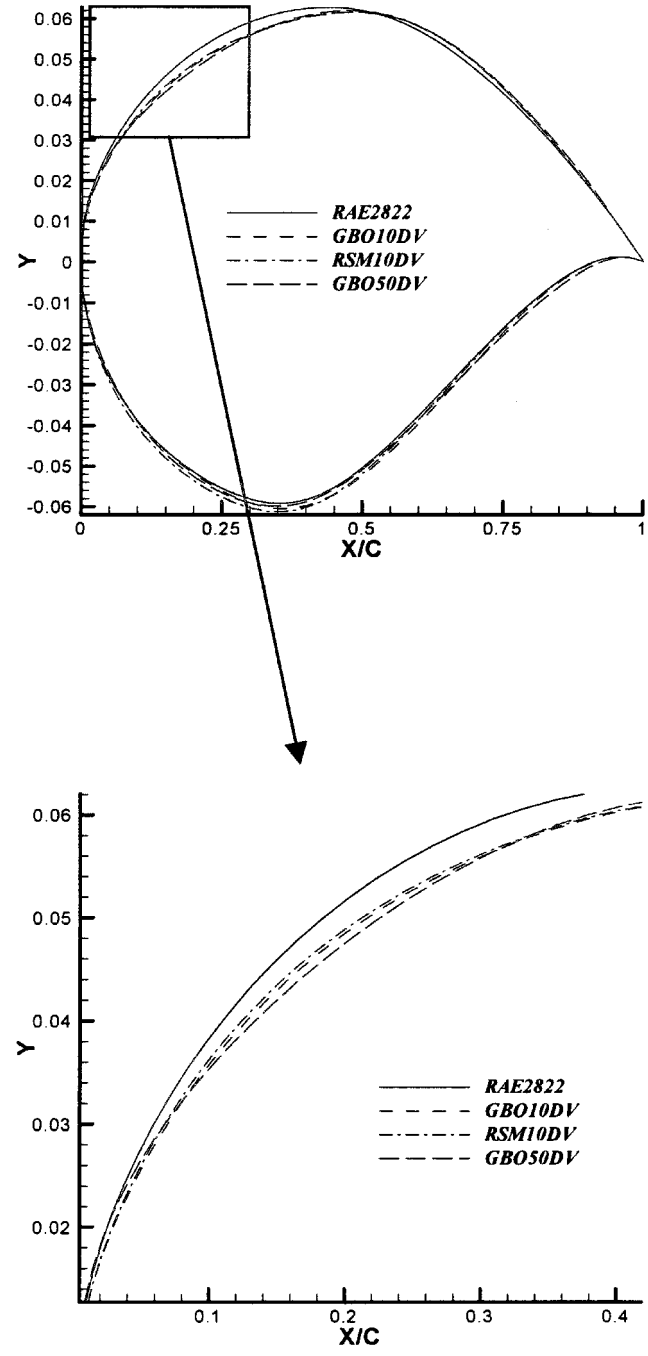

Fig. 4 Airfoil shapes comparison of GBO50DV, RSM10DV, and GBO10DV.

the variation ranges may have negative effect on the fitting quality of the response surface model. Therefore, two design variables, $x11$ and $x12$ are added as shown in Fig. 2 to the set of 10 design variables at the leading-edge region of upper surface to allow more drastic variation of the leading-edge geometry.

For the RSM12DV case, 201 experiments are performed to construct response surface models, the fitting ability of which is shown in Table 4. Although the same range of design variables for the RSM10DV is used, R^2 and adjusted-R^2 values are somewhat decreased and %RMSE is increased compared with those of RSM10DV case. This suggests that the additional two design variables have drastically increased the nonlinear characteristics of the objective function and the constraint.

Figure 5 compares airfoil shapes and pressure distributions of optimized airfoils by GBO12DV, RSM12DV, and GBO50DV. The designed airfoil by RSM12DV is similar to the airfoil by GBO50DV. On the other hand, the one by GBO12DV does not show improvement over the result of GBO10DV case.

Table 5 Summary of aerodynamic performances of optimized airfoils

Airfoil	C_l	C_d	Area	Solver time
RAE2822	0.7894	0.01928	0.07780	——
GBO50DV	0.7894	0.01510	0.07785	(146, 32) = 210
RSM10DV	0.7897	0.01616(0.01615)	0.07815	121
RSM12DV	0.7802	0.01527(0.01546)	0.07780	201
GBO10DV	0.7866	0.01573(0.01579)	0.07781	(24, 2) = 28
GBO12DV	0.7889	0.01582(0.01583)	0.07660	(23, 2) = 27

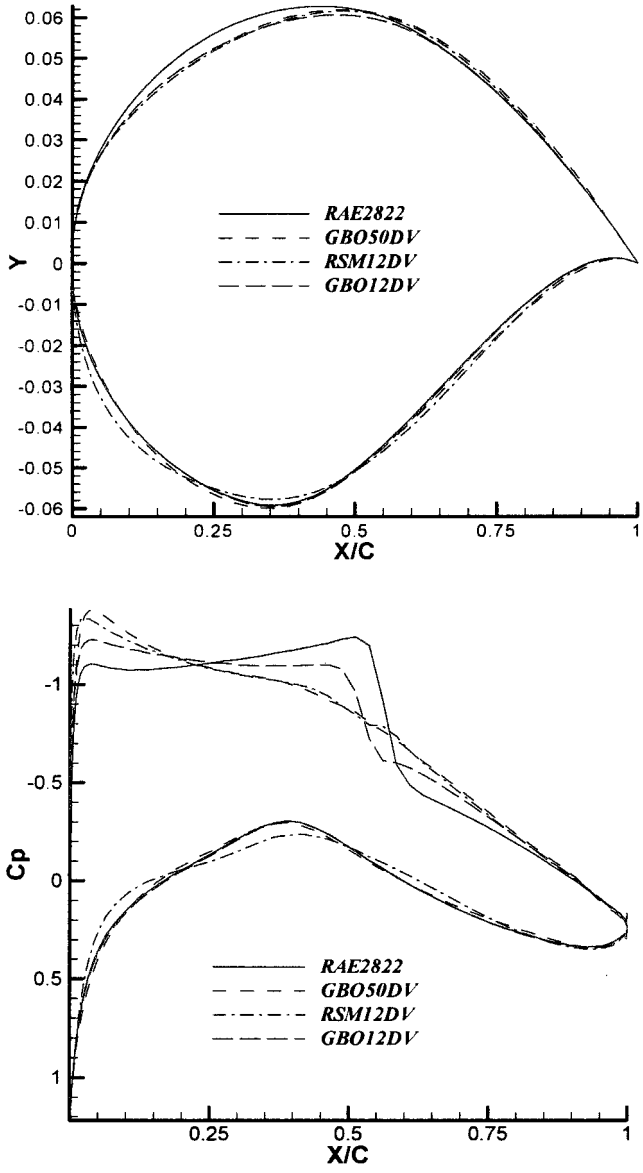

Fig. 5 GBO50DV, RSM12DV, and GBO12DV.

Although the RSM12DV is not fitted with a quadratic function as closely as the RSM10DV, note that RSM can find the value near the global optimum in a nonlinear design space with 12 design variables. However, the GBOM result is still far from the global one. We can also conclude that the RSM can design a shock-free airfoil with fewer design variables than GBOM. This enables the overall computational cost in MDO problems to be reduced and renders the design space so simple that design results can be improved further. The aerodynamic performances of designed airfoils are summarized in Table 5.

Because the constructed response surface has an inherent prediction error in RSM, and because lift constraint in GBOM is imposed as a penalty form, the lift coefficients by both methods do not satisfy the constraint exactly. GBO12DV does not satisfy the area constraint and has a higher drag coefficient than GBO10DV. When the number of design variables is less than 12, the overall computational cost of RSM is $5 \sim 10$ times that of GBOM with the same number of design variables. However, GBO50DV requires slightly more computational cost than RSM12DV. This is because the increase of the number of design variables makes the GBOM numerically ill conditioned and requires much more design iteration near the optimum solution.

From the results of the study on the number of design variables, we can state that RSM with 12 design variables has the competitive edge over GBOM with 50 design variables for the performance of the design airfoils and the required computational cost when locations and the ranges of design variables are carefully selected. Besides, because the number of design variables needed to yield the best solutions are reduced in RSM, it is confirmed that RSM can effectively be applied to MDO problems in the transonic turbulent flow regime. This would reduce overall computational cost in MDO problems, and the overall design results would be improved further with the reduced dimension of design space.

Constraint Imposition Methods

In this section, geometric constraints (i.e., the area constraint and the maximum thickness constraint) are considered. Two

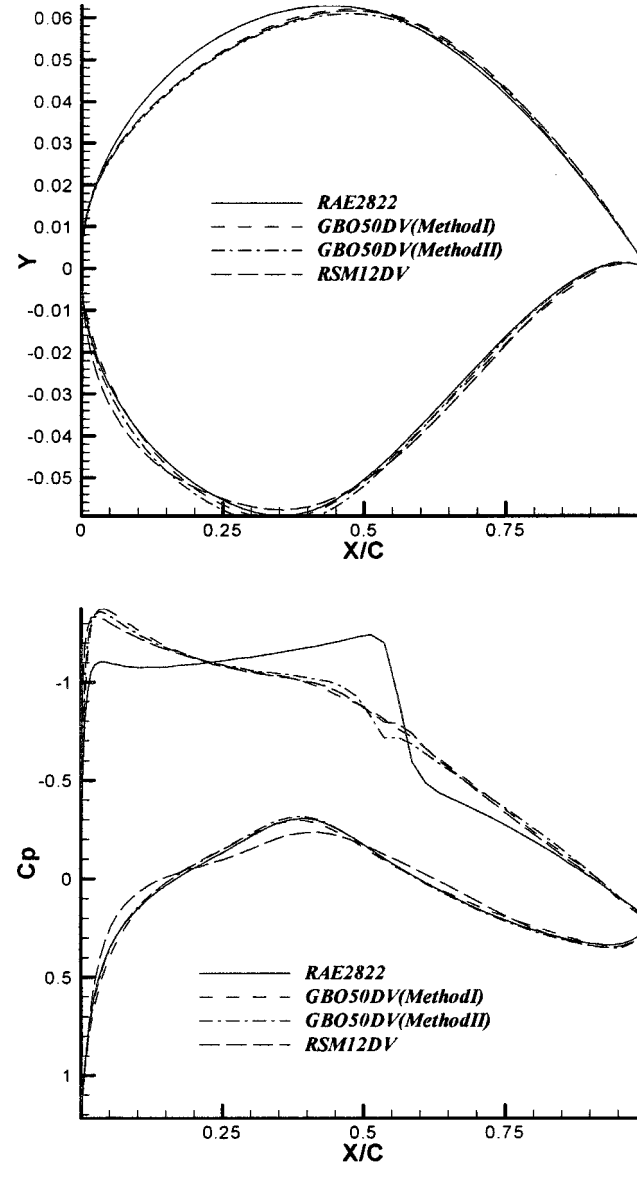

Fig. 6 Airfoil shapes and pressure distributions with area constraints.

different constraint imposition methods for GBOM are tested as follows:

Method 1: minimize $F = F_0 + 10 \cdot \max(\text{Area} - \text{Area}_0, 0)$

or $F = F_0 + 10 \cdot \max(\text{Maxthickness} - \text{Maxthickness}_0, 0)$

Method 2: minimize $F = F_0$ subject to G $\text{Area}_0 - \text{Area} \leq 0$

or $G = \text{Maxthickness}_0 - \text{Maxthickness} \leq 0$ (17)

where $F_0 = 10 \cdot C_d + \max(C_{l_0} - C_l, 0)$.

In method 1, the design problem becomes an unconstrained one when the constraint in the objective function is considered a penalty function term with a mild penalty factor. This may cause the design results to slightly violate the constraint.

In method 2, on the other hand, the constraint is imposed with a constrained design option in DOT to meet exactly the constraint.

Throughout, optimization process gradients of the area constraint are constant, but those of the maximum thickness constraint vary because the maximum thickness position may change. However, the difference in both constraints does not make much difference in final airfoil geometry.

Table 6 shows the design results with the area constraint. The GBOM results by both methods satisfy the constraint. Method 1 gives the best aerodynamic performance at a cost of the largest computational time.

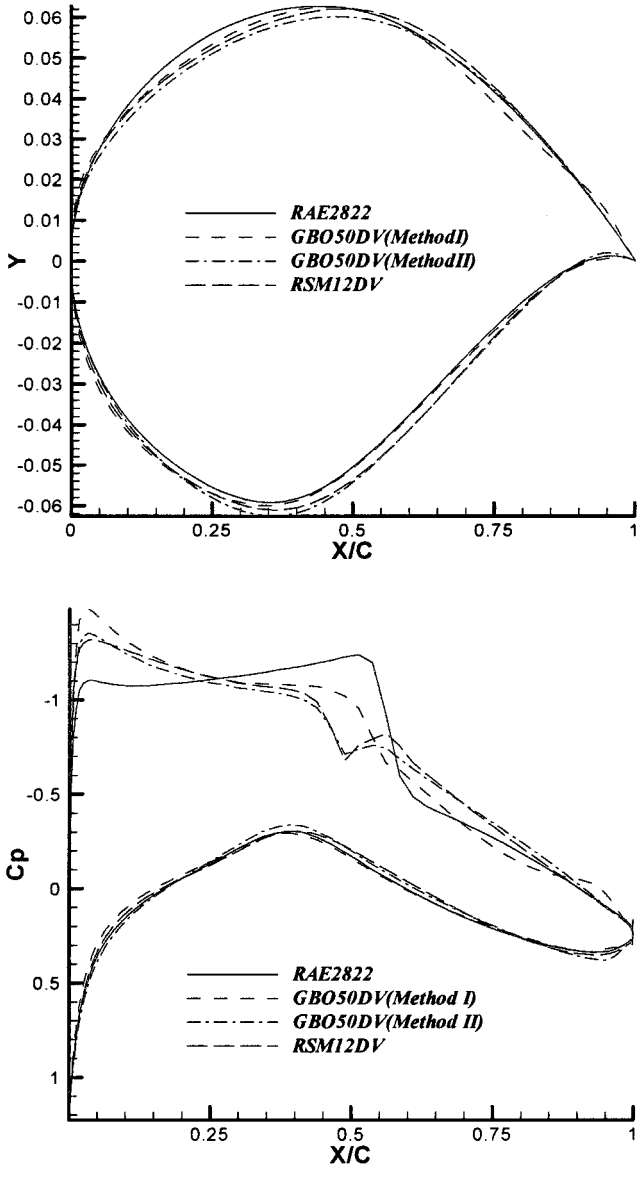

Fig. 7 Airfoil shapes and pressure distributions with maximum thickness constraint.

Table 6 Comparison of design results with area constraint

Airfoil	C_l	C_d	Area	Solver time
RAE2822	0.7894	0.01928	0.07780	——
GBO50DV (method 1)	0.7894	0.01510	0.07785	210
GBO50DV (method 2)	0.7894	0.01526	0.07779	112
RSM12DV	0.7802	0.01527(0.01546)	0.07780	201

Table 7 Comparison of design results with maximum thickness constraint

Airfoil	C_l	C_d	Maximum thickness	Solver time
RAE2822	0.7894	0.01928	0.1210	——
GBO50DV (method 1)	0.7878	0.01596(0.01598)	0.1207	114
GBO50DV (method 2)	0.7713	0.01508(0.01531)	0.1210	295
RSM12DV	0.7788	0.01572(0.01585)	0.1212	201

When the maximum thickness constraint is imposed, as shown in Table 7, method 1 violates the constraint and renders a larger drag coefficient than other design methods. Method 2 gives the best performance in this case, but it also takes the greatest computation time.

Optimized airfoil shapes and corresponding pressure distributions are given in Figs. 6 and 7. When the area constraint is imposed, design results are almost identical with one another, as can be seen in Fig. 6. However, when the maximum thickness constraint is imposed, the results have different shock strengths, shock locations, and airfoil shapes, as shown in Fig. 7.

From these two cases, note that the two methods of geometric constraint specification for the GBOM show different tendencies for the area and maximum thickness constraints. On the other hand, even though RSM is employed with fewer design variables, RSM gives reasonable design results regardless of the characteristics of constraints with acceptable computational cost. Moreover, any change of imposed constraints in RSM does not require additional computational experiments.

Conclusions

The work presented in this paper addresses the viability of RSM as an alternative design tool in the transonic flow regime where a nonsmooth and noisy objective function with constraints exists. Comparisons are made between RSM and GBOM for various sets of design variables and geometric constraint specification methods.

Although RSM has limitations on the number of design variables due to the computational cost, the method is found to yield a shock-free airfoil with a much smaller number of design variables than GBOM. The design results by GBOM using the adjoint method are not improved in proportion to the number of design variables.

In contrast, RSM gives robust solutions regardless of the form of the constraints, whereas GBOM results highly depend on the form of the geometric constraints.

These observations imply that RSM still retain the generally known advantages of being in the transonic regime and that RSM could be a versatile tool in transonic aerodynamic design and MDO problems at any flow speed regimes.

Acknowledgments

We gratefully acknowledge the support of Center of Innovative Design Optimization Technology (Engineering Research Center of Korea Science and Engineering Foundation) and the Brain Korea 21 project.

References

[1]Narducci, R., Grossman, B., Valorani, M., Dadone, A., and Haftka, R. "Optimization Methods for Nonsmooth or Noisy Objective Functions in Fluid Design Problems," AIAA Paper 95-1648, Jan. 1995.

[2]Eyi, S., Lee, K. D., Rogers, S. E., and Kwak, D., "High Lift Design Optimization Using the Navier–Stokes Equations," AIAA Paper 95-0477, Jan. 1995.

[3]Lee, K. D., and Eyi, S., "Aerodynamic Design via Optimization," *Journal of Aircraft*, Vol. 29, No. 6, 1992, pp. 1012–1019.

[4]Chang, I., Toress, F. J., Driscoll, F. P., and van Dam, C. P., "Optimization of Wing–Body Configuration by the Euler Equations," AIAA Paper 94-1899, June 1994.

[5]Guinta, A. A., "Aircraft Multidisciplinary Design Optimization Using Design of Experimental Theory and Response Surface Modeling Methods," Ph.D. Dissertation, Dept. of Aerospace Engineering, Virginia Polytechnic Inst. and State Univ., Blacksburg, VA, May 1997.

[6]Burgee, S., Guinta, A. A., Balalbanov, V., Grossman, B., Mason, W. H., Narducci, R., Haftka, R. T., and Watson, L. T., "A Coarse-Grained Parallel Variable-Complexity Multidisciplinary Optimization Paradigm," *International Journal of Supercomputer Applications and High Performance Computing*, Vol. 10, No. 4, 1996, pp. 269–299.

[7]Jameson, A., Pierce, N. A., and Maritnelli, L., "Optimum Aerodynamic Design Using the Navier–Stokes Equations," AIAA Paper 97-0101, Jan. 1997.

[8]Mohammadi, B., "Optimal Shape Design, Reverse Mode of Automatic Differentiation and Turbulence," AIAA Paper 97-0099, Jan. 1997.

[9]Male, J. M., Mohammadi, N., and Schmidt, R., "Direct and Reverse Modes of Automatic Differentiation of Programs for Inverse Problems," Application to Optimum shape Design, *Proceedings of the 2nd International SIAM Workshop on Computational Differentiation*, Santafe, 1996.

[10]Kim, H. J., Kim, C., Rho, O. H., "Aerodynamic Sensitivity Analysis for Navier–Stokes Equations," AIAA Paper 99-0402, Jan. 1999.

[11]Hwang, S. W., "Numerical Analysis of Unsteady Supersonic Flow over Double Cavity," Ph.D. Dissertation, Dept. of Aerospace Engineering, Seoul National Univ., Seoul, Republic of Korea, Feb. 1996.

[12]Kim, H. J., and Rho, O. H., "Dual-Point Design of Transonic Airfoils Using the Hybrid Inverse Optimization Method," *Journal of Aircraft*, Vol. 34, No. 5, 1997, pp. 612–618.

[13]Vanderplaats, G. N., and Hansen, S. R., *DOT USERS MANUAL*, VMA Engineering, Goleta, CA, 1989.

[14]Myers, R. H., and Montgomery, D. C., *Response Surface Methodology: Process and Product Optimization Using Designed Experiments*, Wiley, New York, 1995, pp. 1–141, 279–401, 462–480.

[15]Ahn, J., Yee, K., Lee, D.-H., "Two-Point Design Optimization of Transonic Airfoil Using Response Surface Methodology," AIAA Paper 99-0403, Jan. 1999.